DOI: 10.1002/ejic.200600198

Luminescent Open-Framework Antiferromagnet – Hydrothermal Syntheses, Structures, and Luminescent and Magnetic Properties of Two Novel Coordination Polymers: $[Zn(pdoa)(bipy)]_n$ and $\{[Mn(pdoa)(bipy)](bipy)\}_n$ [pdoa = 2,2′-(1,3-phenylenedioxy)bis(acetate); bipy = 4,4′-bipyridine]

Xian-Lan Hong,[a,b] Junfeng Bai,*[a] You Song,[a] Yi-Zhi Li,[a] and Yi Pan*[a]

Keywords: Functional coordination polymers / Polycarboxylate ligands / 4,4′-Bipyridine / Luminescence

Two coordination polymers of mixed ligands, 2,2′-(1,3-phenylenedioxy)bis(acetate) (pdoa) and 4,4′-bipyridine (bipy), namely $[Zn(pdoa)(bipy)]_n$ (**1**) and $\{[Mn(pdoa)(bipy)](bipy)\}_n$ (**2**), have been hydrothermally synthesized and characterized by single-crystal X-ray diffraction and IR spectra. Complex **1** crystallizes in the triclinic space group $P\bar{1}$ with a = 6.8826(18) Å, b = 11.202(3) Å, c = 12.295(3) Å, α = 86.854(4)°, β = 85.759(5)°, γ = 72.629(4)° and is a novel folded-paper-shaped coordination compound with polymeric sheets formed by the five-coordinate Zn^{II} centers and bridging pdoa and bipy. Complex **2** crystallizes in the monoclinic space group $P2_1/c$ with a = 11.507(2) Å, b = 23.254(5) Å, c = 9.8710(19) Å, β = 96.418(4)° and exhibits a robust three-dimensional framework with nanosized rectangular channels (11.627 × 11.507 Å). They both display blue fluorescent emission and could be considered as new luminescent materials. In addition, the magnetic properties of complex **2** were investigated and the magnetic susceptibility data were rationally fitted with g = 2.072(5), J = –1.11(4) cm^{-1}, and zJ' = –0.161(7) cm^{-1}, showing it is an unprecedented luminescent open-framework antiferromagnet.

Introduction

In recent years, metal-organic coordination polymers based on multicarboxylate ligands have been of great interest because of their fascinating molecular topologies and crystal-packing motifs along with their outstanding properties in spectroscopy, magnetism, and catalysis, and potential applications as functional materials.[1] Much work has been focused on rigid ligands and flexible ligands such as benzenedicarboxylates[2] and aliphatic carboxylates,[3] respectively. However, there are few examples of ligands containing both aromatic and aliphatic features.[4] Moreover, the combination of both dicarboxylate and 4,4′-bipyridine ligands helps to assemble higher-dimensional supramolecular networks.[5] Meanwhile, chemists have been pursuing multifunctional materials for molecule devices. But, to the best of our knowledge, porous coordination networks usually exhibit a single functionality, such as luminescence or magnetic ordering.[6–9]

[a] State Key Laboratory of Coordination Chemistry & School of Chemistry and Chemical Engineering, Nanjing University, Nanjing 210093, P. R. China
E-mail: bjunfeng@nju.edu.cn
yipan@nju.edu.cn
[b] School of Public Health and Tropical Medicine, Southern Medical University,
Guangzhou 510515, P. R. China
E-mail: hongxianlan@yahoo.com.cn

We are interested in the utilization of polycarboxylate ligands with characteristics of both flexibility and rigidity, such as 2,2′-(1,4-phenylenedioxy)bis(acetate) and 2,2′-(1,3-phenylenedioxy)bis(acetate), which were initially investigated as herbicides and remained almost unexplored in the field of crystal engineering and supramolecular chemistry to construct coordination polymers.[10] The $–OCH_2–$ group makes these ligands more flexible in comparison with the corresponding benzenedicarboxylate, whilst the existence of the benzene ring provides a rigid element. Herein, we report hydrothermal syntheses, crystal structures, and solid-state photoluminescent and magnetic properties of two novel coordination polymers with mixed ligands, 2,2′-(1,3-phenylenedioxy)bis(acetate) (pdoa) and 4,4′-bipyridine (bipy), $[Zn(pdoa)(bipy)]_n$ (**1**) and $\{[Mn(pdoa)(bipy)](bipy)\}_n$ (**2**), in which complex **1** is an interesting 2D folded-paper-shaped structure, whereas complex **2** is an intriguing 3D framework structure with rectangular nanosized channels. Both, **1** and **2** display blue fluorescent emission, and complex **2** exhibits the characteristics of a weak antiferromagnetic coupling between metal ions in the system mediated by both types of the bridging ligands. Interestingly, to the best of our knowledge, complex **2** is the first example of an open-framework coordination polymer with conjugation of blue fluorescent emission and antiferromagnetic long-range ordering.

Results and Discussion

Description of the Crystal Structures

The asymmetric unit of compound **1** contains one Zn^{2+} ion, one 2,2′-(1,3-phenylenedioxy)bis(acetate) ligand, and two half bipy molecules (Figure 1a). The zinc ion is five-coordinate in a distorted square-pyramidal environment of asymmetry with three oxygen atoms of two different carboxylate groups, one bipy nitrogen atom in the basal plane (O1, O2, O5, N2), and one nitrogen atom of another bipy ligand at the apex position (N1). Two carboxylate groups in the same pdoa molecule have different coordination modes, in which one acts as a chelating bidentate and the other serves as a monodentate ligand. The unequal coordination of two oxygen atoms (O1 and O5) from the chelating bidentate carboxylate moiety of pdoa results from the asymmetrical five-coordination environment. From the crystallographic data and selected bond lengths and angles for the title complexes (Tables 1 and 2), the lengths of Zn1–O1 [2.244(2) Å] and Zn1–O5 [2.131(2) Å] are similar to those, relative to the chelating bidentate carboxylate ligand, found in $[Zn_3(Hcit)_2(H_2O)_2]_n$ [2.318(2)–2.071(2) Å][11a] and $[Zn_4(OH)_2(fa)_3(bipy)_2]$ [2.367(4)–2.089(4) Å][11b] (Hcit and fa denote citric acid anion and fumarate, respectively). However, the separation of Zn1 from O2 of the monodentate COO^- group [Zn1–O2 1.9369(18) Å] is significantly shorter than those relative to the chelating bidentate carboxylate ligand, but consistent with those referring to the monodentate carboxylate ligand in $[Zn_3(\mu_3\text{-}OH)(\mu_2\text{-}OH)(bipy)_{0.5}(oba)_2]\cdot 0.5H_2O$ [1.939(4) Å, oda = 4,4′-oxybis-(benzoate)][11c] and $[Zn_3(Hcit)_2(H_2O)_2]_n$ [2.028(2) Å],[11a] implying the existence of a certain tension in the four-membered ring formed between the chelating bidentate COO^- group and the zinc ion. The Zn–N distances [Zn1–N1 2.048(2) Å and Zn1–N2 2.090(2) Å] are slightly shorter than those in structurally related polymers $[Zn(tp)(4,4'\text{-bipy})]_n$ [2.154(2) and 2.186 Å] (tp denotes terephthalate).[12] The Zn^{2+} ions are linked by pdoa ligands forming infinite straight-linear chains along the *b*-axis. Furthermore, such linear chains are bridged at the point of Zn^{2+} ions by bipy ligands to form two-dimensional sheets (Figure 2a), which have an interesting folded-paper-like topology as illustrated in Figure 2b. The two pyridine rings of the bipy molecule are almost coplanar (dihedral angle about 0.93°) and there is an inversion center at the midpoint of the C1–C1′ bond of each bipy ligand. The adjacent Zn···Zn distance due to the pdoa ligand in the same chain is 11.202(3) Å and the Zn···Zn distance between adjacent chains due to bipy is 11.170 (2) Å. Furthermore, the resulting 2D wave-like sheets superpose on each other with crest to crest, forming a 3D supramolecular lattice of noninterpenetration by weak C–H···O H bonds [C17#1–H17#1···O20 or C17–H17···O20#1, with a C···O distance of 3.468 Å and a C–H···O angle of 148.86°; symmetry code: #1: $1 - x$, $1 - y$, $1 - z$] and the offset face-to-face π–π stacking interactions between the pyridine ring of bipy and the phenyl ring of pdoa (represented as *α* and *β* in Figure 3, respectively, with a separation of 3.397 Å from *α* to *β*, and with an angle of 164.1° between them). These weak H bonds and π–π interactions are important in the construction of supramolecules, as is well documented in the literature.[13] Another interesting feature of the structure is that the pdoa ligands jut out and stand on the crests of folded-paper-like sheets, filling the voids among the layers (Figure 3).

As shown in Figure 1b, the asymmetric unit of complex **2** contains one Mn^{2+} ion, one pdoa ligand, one coordinated, and one free bipy molecule. The Mn atom is in an octahedral environment with two bipy nitrogen donors (N1, N2#3) occupying the axial positions and four oxygen atoms (O2, O3#2, O5#4, O6#1) from four different pdoa ligands in the equatorial plane (symmetry codes: #1: $-1 + x$, y, $-1 + z$; #2: x, $1.5 - y$, $-0.5 + z$; #3: $1 - x$, $0.5 + y$, $0.5 - z$; #4: $-1 + x$, $1.5 - y$, $-0.5 + z$). The two pyridine rings of each coordinated or guest bipy molecule are not coplanar, and twisted around each other with dihedral angles 6.63(2)° and 6.75(2)° for coordinated and guest bipy, respectively, in contrast to those in complex **1** in which they are virtually coplanar. The axial Mn–N distances [Mn–N1 2.386(3);

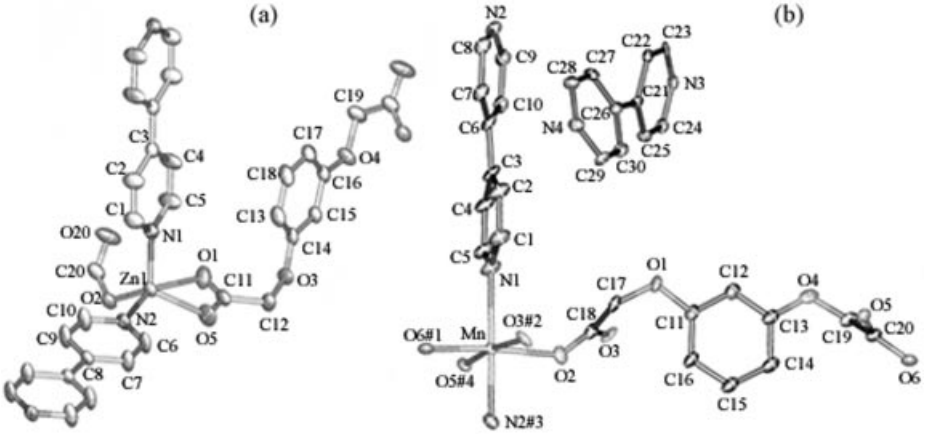

Figure 1. Structural plots showing the asymmetric unit and the metal ion's coordination environment for complexes **1** (a) and **2** (b); thermal ellipsoids are drawn at 30% probability and all the H atoms are omitted for clarity (symmetry codes: #1: $-1 + x$, y, $-1 + z$; #2: x, $1.5 - y$, $-0.5 + z$; #3: $1 - x$, $0.5 + y$, $0.5 - z$; #4: $-1 + x$, $1.5 - y$, $-0.5 + z$).

Table 1. Crystal data and details of the structure determination for complexes **1** and **2**.

	1	**2**
Empirical formula	$C_{20}H_{16}N_2O_6Zn$	$C_{30}H_{24}MnN_4O_6$
Formula mass	445.74	591.47
Crystal system	triclinic	monoclinic
Space group	$P\bar{1}$	$P2_1/c$
b [Å]	11.202(2)	23.254(5)
c [Å]	12.295(3)	9.8710(19)
α [°]	86.854(4)	90
β [°]	85.759(5)	96.418(4)
Z	2	4
V [Å^3]	901.7(4)	2624.7(9)
$d_{calcd.}$ [g cm^{-3}]	1.642	1.497
μ [mm^{-1}]	1.405	0.557
F (000)	456	1220
Crystal size [mm]	0.30×0.30×0.20	0.32×0.22×0.18
θ range [°]	2.49–28.02	1.75–26.00
Reflections collected	5344	14053
Unique reflections	3954 [R(int) = 0.0730]	5149 [R(int) = 0.0258]
R indices [$I > 2\sigma(I)$]	R_1 = 0.0442, wR_2 = 0.1158	R_1 = 0.0489, wR_2 = 0.1079
R indices (all data)	R_1 = 0.0485, wR_2 = 0.1182	R_1 = 0.0742, wR_2 = 0.1151

Table 2. Selected bond lengths [Å] and angles [°] for complexes **1** and **2**.[a]

1			
Zn1–O1	2.244(2)	Zn1–O2	1.9369(18)
Zn1–O5	2.131(2)	Zn1–N1	2.048(2)
Zn1–N2	2.090(2)		
O1–Zn1–O2	100.70(8)	O1–Zn1–O5	59.11(8)
O1–Zn1–N2	149.44(9)	O2–Zn1–O5	133.92(10)
O2–Zn1–N1	116.57(8)	O2–Zn1–N2	97.15(8)
O5–Zn1–N1	106.05(10)	O5–Zn1–N2	90.75(8)
O1–Zn1–N1	92.71(9)	N1–Zn1–N2	101.23(8)
2			
Mn–O(6)#1	2.108(2)	Mn–O(3)#2	2.1422(17)
Mn–N(2)#3	2.164(2)	Mn–O(2)	2.2044(19)
Mn–O(5)#4	2.2379(18)	Mn–N(1)	2.386(3)
O(6)#1-Mn–O(3)#2	92.63(7)	O(6)#1-Mn–N(2)#3	85.42(8)
O(3)#2-Mn–N(2)#3	88.25(8)	O(6)#1-Mn–O(2)	174.60(7)
O(3)#2-Mn–O(2)	86.24(7)	N(2)#3-Mn–O(2)	89.27(8)
O(6)#1-Mn–O(5)#4	93.08(7)	O(3)#2-Mn–O(5)#4	172.66(7)
N(2)#3-Mn–O(5)#4	87.62(7)	O(2)–Mn–O(5)#4	87.65(7)
O(6)#1-Mn–N(1)	92.55(8)	O(3)#2-Mn–N(1)	88.62(8)
N(2)#3-Mn–N(1)	176.19(8)	O(2)–Mn–N(1)	92.70(8)
O(5)#4-Mn–N(1)	95.73(7)		

[a] Symmetry codes: #1: –1 + x, y, –1 + z; #2: x, 1.5 – y, –0.5 + z; #3: 1 – x, 0.5 + y, 0.5 – z; #4: –1 + x, 1.5 – y, –0.5 + z.

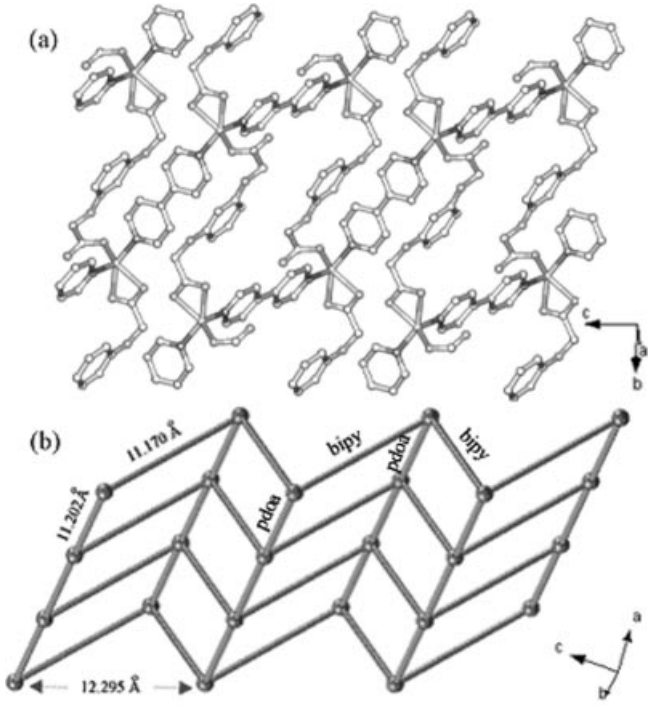

Figure 2. (a) Schematic illustration of the 2D network with all the H atoms omitted for clarity; (b) folded-paper-like topologic diagram of $[Zn(pdoa)(bipy)]_n$ (gray spheres denote zinc atoms).

Mn–N2#3 2.164(2)] and the Mn–O distances [Mn–O2 2.2044(19) Å; Mn–O3#2 2.1422(17) Å; Mn–O5#4 2.2379(18) Å; Mn–O6#1 2.108(2) Å] are comparable to those of analogous complexes,[14] indicating the manganese asymmetric coordination environment in terms of diversities of bond strength. All the carboxylate groups act as bis(unidentate) ligands and each pdoa ligand links four different manganese ions to form an equatorial $[Mn(pdoa)]_n$ sheet (Figure 4a), in which all the phenyl rings are parallel to each other and vertical to the crystallographic *ac* plane. The Mn···Mn separation due to pdoa is 11.507(3) Å, significantly larger than that of $[Mn(5\text{-methylpyrazole})_2(tp)]_n$ (9.655–9.659 Å) based on a tp ligand.[14b] It can be easily seen, from the view of the $[Mn(pdoa)]_n$ layer along the *c*-axis (Figure 4b), that all the manganese ions are not in one plane, instead alternatively situated above and below the plane between them. Interestingly, as shown in Figure 4a, this sheet contains distinctive duplex helixes of –Mn–O–C–O–Mn– with $Mn(O–C–O–)_2Mn$ eight-membered rings; the Mn···Mn distance relative to the bridging carboxylate group is 4.999(2) Å, similar to that of $[Mn(5\text{-methylpyrazole})_2(tp)]_n$ (4.917 Å),[14b] and shorter than that of $[Mn(bipy)(H_2O)(C_4H_4O_4)]\cdot 0.5bipy$ [5.264(1) Å, $C_4H_4O_4$ = succinate dianion].[14c] The analogous duplex helix was found in $Tb(bdc)NO_3\cdot 2DMF$ (bdc = 1,4-benzenedicarboxylate).[15]

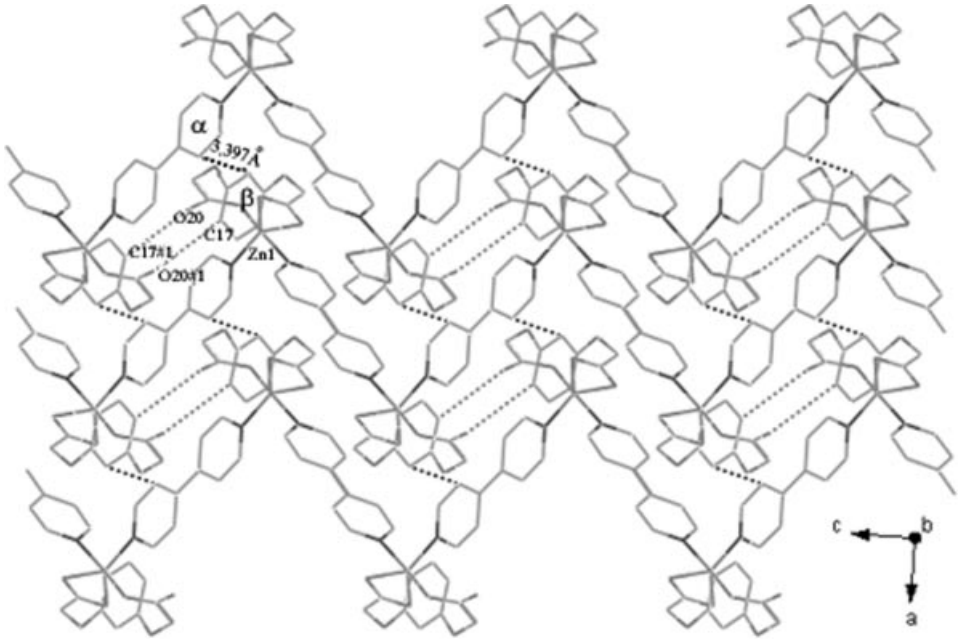

Figure 3. Perspective view along the *b*-axis of complex **1** showing the weak C–H···O H bonds (gray dotted lines) and the offset face-to-face π–π stacking interactions (dark gray dotted lines) between the puckered layers. All the H atoms have been omitted for clarity (symmetry code: #1: 1 – *x*, 1 – *y*, 1 – *z*).

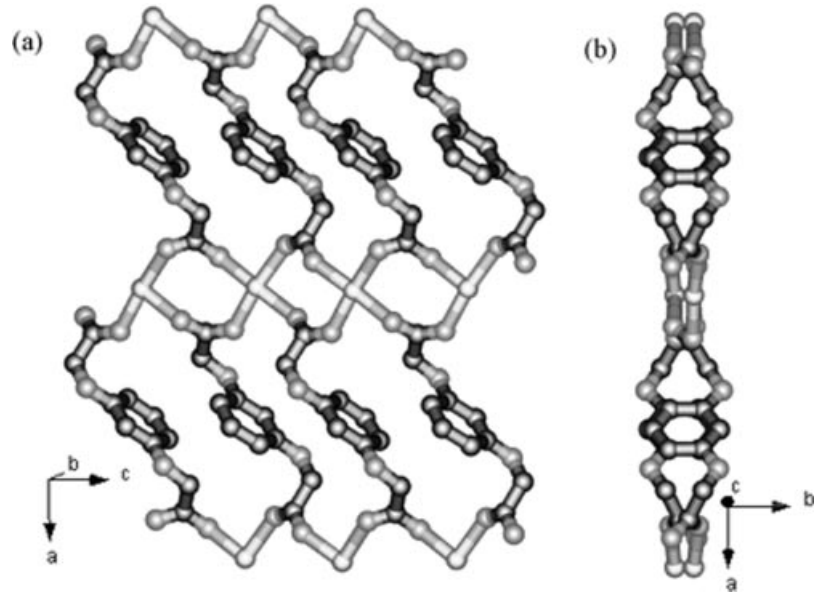

Figure 4. (a) Representation of the $[Mn(pdoa)]_n$ plane in complex **2**. (b) View of the $[Mn(pdoa)]_n$ plane in complex **2** along the *c*-axis. All hydrogen atoms have been omitted for clarity.

It is noteworthy that such a uniform Mn^{II} carboxylate 2D sheet with only one coordination mode of the carboxylate moiety acting as bis(unidentate) bridging ligand to connect four metal ions in complex **2** is unprecedented.

Furthermore, the $[Mn(pdoa)]_n$ sheets are pillared by the rigid μ-4,4′-bipyridine ligands to form a 3D open framework exhibiting one-dimensional rectangular tunnels along the *c*-axis with dimensions of 11.627 × 11.507 Å (Figure 5a), which is considerably larger than that of reported manganese analogues.[14a,14c] To the best of our knowledge, this manganese inorganic-organic hybrid polymer with a noninterpenetration three-dimensional framework exhibits the largest channel among similar Mn^{II} pillar-layered structures documented to date.[14]

The free bipy ligands as guest molecules and templates, like the examples,[16] reside at the 1D channel (Figure 5b). Unfortunately, removing the guest bipy molecules will give rise to collapse of the framework and decomposition of the whole complex, which was confirmed by thermal gravimetric analyses. Moreover, there exist weak H bonds between the guest and coordinated bipy molecules, as represented in Figure 5b, C4#5–H4#5···N3 and C4#7–H4#7···N3#6

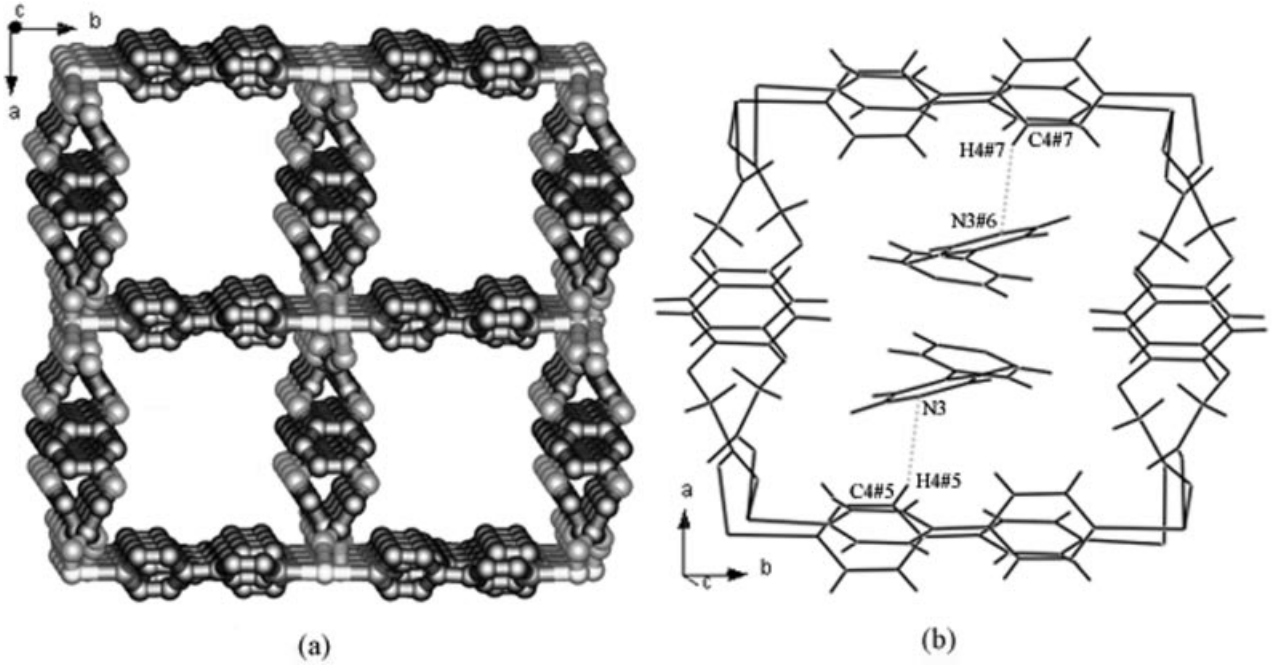

Figure 5. (a) Projection of the 3D network showing the rectangular channels along the *c*-axis in complex **2**. All hydrogen atoms and guest 4,4′-bipyridine molecules have been omitted for clarity. (b) A part of the side view of the 3D structure of **2** showing the guest 4,4′-bipyridine molecules residing at the 1D channel and the weak H bonds (C–H···N, shown as gray dotted lines) between the coordinated and guest 4,4′-bipyridine molecules (symmetry codes: #5: 1 – *x*, 1 – *y*, 1 – *z*; #6: 2 – *x*, 1 – *y*, 1 – *z*; #7: 1 + *x*, *y*, *z*).

(symmetry codes: #5: 1 – *x*, 1 – *y*, 1 – *z*; #6: 2 – *x*, 1 – *y*, 1 – *z*; #7: 1 + *x*, *y*, *z*); the C···N distance and the angle of C–H···N are 3.30 Å and 146.05°, respectively.

IR Spectrum

As well documented in the literature,[17] IR spectra are very helpful in diagnosing characteristic coordination modes of carboxylate groups and determining the whole structure of previously unknown carboxylate complexes. The crystal structures provide us with an opportunity to investigate the IR spectral characters of pdoa complexes with three coordination modes [unidentate, chelating bidentate, and bridging bis(monodentate)]; representative data of IR spectra for pdoa, **1**, and **2** are tabulated in Table 3. Although the IR spectra of both complexes are complicated because of the overlap of the absorption of pdoa and bipy, several strong bands can be assigned in comparison with those of pdoa, bipy and other related complexes. The absence of the ν(COOH) band at 1762 cm^{-1} and the ν(C–OH) band at 1267 cm^{-1} of H_2pdoa in **1** and **2** suggests that all the carboxylate groups are completely deprotonated. The bands at 3086 and 3048 cm^{-1} for **1** and **2** can be assigned to the C–H stretching vibration of the pdoa ligand in contrast to that of H_2pdoa (3083 cm^{-1}).[18] For complex **1**, the values of ν_{asym}(OCO) and ν_{sym}(OCO) corresponding to the unidentate mode are 1622 cm^{-1} and 1380 cm^{-1} respectively, which are similar to those of some carboxylate complexes with only unidentate coordination of the carboxylate group, such as [Zn(Pht)(py)$_2$] (ν_{asym}: 1618 cm^{-1}; ν_{sym}: 1390 cm^{-1}), [Zn(Pht)(mepy)$_2$] (ν_{asym}: 1622 cm^{-1}; ν_{sym}: 1372 cm^{-1}; here Pht, py, and mepy denote *o*-phthalic dianion, pyridine, and 3-methylpyridine, respectively),[19a] $ZnCl_2$(Hpipe-2)$_2$ (ν_{asym}: 1635 cm^{-1}; ν_{sym}: 1397 cm^{-1}), $ZnCl_2$(Hpipe-3)$_2$·3H_2O (ν_{asym}: 1626 cm^{-1}, ν_{sym} = 1387 cm^{-1}; Hpipe-2 = DL-piperidine-2-carboxylic acid, Hpipe-3 = DL-piperidine-3-carboxylic acid).[19b] However, the values of ν_{asym}(OCO) and ν_{sym}(OCO) relative to those of the chelating bidentate carboxylate group are 1608 cm^{-1} and 1537 cm^{-1}, respectively, similar to those of [Zn(ip)(bipy)$_2$][Zn(ip)(bipy)]·0.25H_2O (ν_{asym}: 1615 cm^{-1}; ν_{sym}: 1555 cm^{-1}; ip = iosphthalate).[19c] Because the COO^- group has only one coordination mode in complex **2**, the very strong absorptions at 1596 and 1407 cm^{-1} are assigned to ν_{asym}(OCO) and ν_{sym}(OCO), which are both highly blue-shifted in comparison with an analogous compound, [Mn(5-methylpyrazole)$_2$(tp)]$_n$ (ν_{asym}: 1558 cm^{-1}; ν_{sym}: 1374 cm^{-1}).[14b] Conclusively, the order of the separation between the asymmetric and symmetric stretching vibrations resulting from complexes **1** and **2** is Δ(unidentate, 242 cm^{-1}) > Δ(bridging bidentate, 189 cm^{-1}) > Δ(chelating bidentate, 71 cm^{-1}), supposing that the effects of variation of metal ions are relatively little to the value of Δ(ν_{asym} – ν_{sym}), which are well in accordance with the documented results of Deacon and Phillips.[17] In addition, the IR characteristics of bipy in complexes **1** and **2** are different. For complex **1**, the two pyridyl rings of bipy acting as a bidentate ligand are almost coplanar. Meanwhile, the bipy molecule has a center of symmetry, as indicated in the X-ray structure, and the in-plane C–H bending vibration (about 1215 cm^{-1}) loses its IR activity. However, for **2**, the two pyridyl rings of each free and coordinated bipy molecule are not coplanar; the IR properties of bipy in **2** are thus similar

Table 3. The data of IR spectra for H_2pdoa and complexes **1** and **2**.

H_2pdoa	3083 (w), 1762 (vs), 1710 (vs), 1596 (vs), 1494 (vs), 1433 (vs), 1340 (m), 1267 (s), 1248 (s), 1192 (vs), 1156 (s), 1087 (vs), 960 (m), 847 (s), 769 (s)
1	3086 (w), 1638 (vs), 1608 (vs), 1537 (s), 1418 (s), 1380 (s), 1292 (s), 1220 (m), 1157 (vs), 1068 (s), 848 (m), 810 (vs), 764 (s), 725 (s), 638 (s)
2	3048 (w), 1596 (vs), 1486 (w), 1407 (vs), 1322 (w), 1283 (s), 1181 (s), 1156 (vs), 1067 (s), 832 (m), 807 (vs), 717 (s), 626 (s), 605 (m)

to those of pyridine. The strong absorption band at 1181 cm^{-1} can be rationally attributed to the in-plane C–H bending vibration of bipy according to the literature.[20]

Luminescent Properties

The excitation and emission spectra for H_2pdoa, $[Zn(pdoa)(bipy)]_n$, and $\{[Mn(pdoa)(bipy)](bipy)\}_n$ are shown in Figure 6. The excitation bands at 350 nm for H_2pdoa could be assigned to π→π* transitions of the O–C_6H_4–O group. Accordingly, the emissions spectra (λ_{ex} = 350 nm) centered approximately at 394 nm can be assigned to the transition emission from the $T_1\pi,\pi^*$ and T_1n,π^* to the ground state of the –OC_6H_4O– group.[21] For complex **1**, the band at 358 nm in the excitation spectra, similar to that of H_2pdoa, is associated with the π→π* transition of the O–C_6H_4–O unit. The band at 473 nm with a shoulder band at 530 nm in the emission spectrum is obviously different to that of H_2pdoa, and accordingly may be assigned to ligand-to-metal charge transfer (LMCT).[11b,11c,22] The excitation and emission spectra of **2** are very similar to those of **1** both in shape and position and are not characteristic of Mn^{2+}, with $3d^5$ electron configuration and octahedral coordination sphere according to the literature,[23] thus the excitation band at 356 nm can be assigned to the π→π* transition of the O–C_6H_4–O group, and the emission at 472 nm with the shoulder band at 535 nm to LMCT. Conclusively, both **1** and **2** may be used as blue-light-emitting functional materials. Complex **2**, with a combination of luminescent and magnetic properties (see below), may especially be a promising candidate for luminescent molecular magnetic materials.

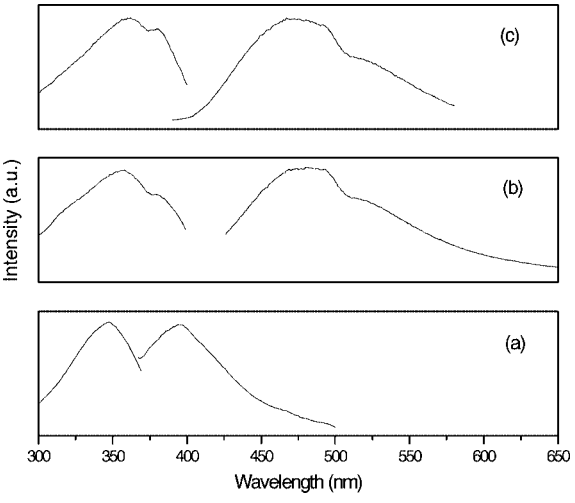

Figure 6. Solid-state excitation-emission spectra of H_2pdoa (a), complex **1** (b), and complex **2** at room temperature (c).

Magnetic Properties

The temperature dependence of the magnetic susceptibility of complex **2** is depicted in Figure 7 in the form of the product $\chi_M T$ versus T in the range of 300–1.8 K. The magnetic susceptibility is corrected for diamagnetism by using Pascal's constants. At room temperature, the product is 4.41 emu K mol^{-1}, which is the same as the spin-only value for Mn^{2+} (s = 5/2 and g = 2.008 determined by EPR). As the temperature is lowered, the product $\chi_M T$ decreases steadily in the whole temperature range to 0.4 emu K mol^{-1} at 1.8 K, indicating the antiferromagnetic interaction between Mn^{II} ions through both bridging ligands bipy and carboxylate. Equally, a maximum was observed in the plot of χ_M versus T (Figure 7), which is the nature of antiferromagnetic coupling between Mn^{II} ions. The magnetic susceptibility data were fitted assuming that the carboxylate bridges between Mn^{II} ions form a uniform chain with exchange constant J and then bipy and pdoa connect the chains to form the 3D structure of this complex with an exchange constant zJ'. Thus, the expression in the literature can be written as Equations (1) and (2) for the magnetic fittings,[24] where $u = \coth[JS(S+1)/kT] - kT/JS(S+1)$.

$$\chi_{chain} = \frac{Ng^2\beta^2}{3kT}\frac{1+u}{1-u}S(S+1) \quad (1)$$

$$\chi_M = \frac{\chi_{chain}}{1-\chi_{chain}(2zJ'/Ng^2\beta^2)} \quad (2)$$

The best parameters obtained by a standard least-squares fitting were g = 2.072(5), J = –1.11(4) cm^{-1}, and zJ' = –0.161(7) cm^{-1} with $R = 4.3\times10^{-6}$ [$R = \sum|(\chi_M)_{exp} - (\chi_M)_{calc}|^2/\sum(\chi_M)^2_{exp}$]. Thus, the bipy and pdoa ligands mediate the very weak antiferromagnetic interaction between the Mn^{II} ions in this system.

For a 3D antiferromagnetic complex, an observed maximum in the plot of χ_M versus T implies the presence of a possible long-range anriferromagnetic ordering. It is confirmed by the specific heat (C_p) determination with a physical property measurement system (PPMS) at 10^{-4} Torr and zero field. The total specific heat (C_p) of complex **2** at low temperatures in the range of 1.8–8.5 K was determined ex-

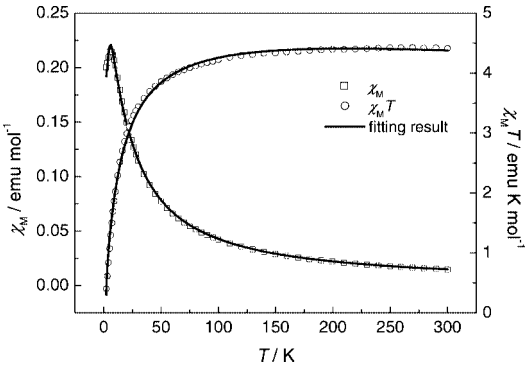

Figure 7. Temperature dependence of magnetic properties of complex **2** in the form of $\chi_M T$ (○) vs. T and χ_M (□) vs. T; the solid line is the fitting of experimental data.

perimentally and the result is shown in Figure 8. It is accepted that the lattice-specific heats generally vary smoothly with the temperature and are not influenced greatly by the details of the structure. Therefore, we can gain insight into the magnetic properties from the variance of the total specific heat with the change of temperature. As seen in Figure 8, a peak is observed at 1.9 K and the lambda shape is similar to those of some one-dimensional antiferromagnetic compounds, such as $CsMnCl_3 \cdot 2H_2O$, MnF_2, and $(CH_3)_4NMnCl_3$.[25] The plot of C_p versus T further confirms the antiferromagnetic interaction between the Mn^{II} ions in complex **2**; there is long-range ordering below 1.9 K (Neel temperature). Similar behavior was found in $[Mn_2(pm)]$, where pm represents 1,2,4,5-benzenetetracarboxylate.[26] To the best of our knowledge, complex **2** represents the first example of an open-framework coordination polymer with conjugation of blue fluorescent emission and antiferromagnetic long-range ordering, a promising candidate for multifunctional materials, such as luminescent molecular magnetic materials.

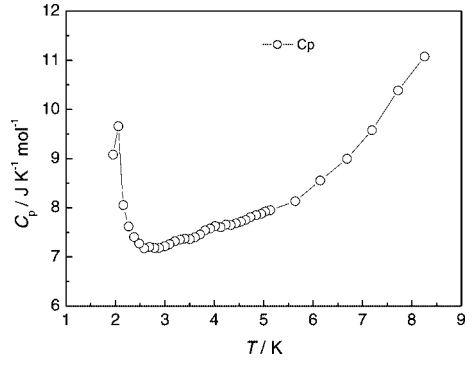

Figure 8. Total specific heat, C_p, plotted against temperature, T, for complex **2** between 1.8 and 8.5 K.

Conclusions

Two coordination polymers containing 2,2′-(1,3-phenylenedioxy)bis(acetate) (pdoa) and 4,4′-bipyridine (bipy) with formulae $[Zn(pdoa)(bipy)]_n$ (**1**) and $\{[Mn(pdoa)(bipy)](bipy)\}_n$ (**2**) have been synthesized and characterized by single-crystal X-ray diffraction analyses and IR spectra and their luminescent properties and the magnetic behaviors have been investigated. The reactions of $ZnCl_2$ and $Mn(OOCCH_3)_2$ with pdoa and bipy under the same conditions result in strikingly different structures. Complex **1** has an interesting 3D noninterpenetration supramolecular structure, whereas complex **2** forms under the same reaction conditions an intriguing 3D open-framework structure with rectangular nanosized channels. The order of the separation between the asymmetric and symmetric stretching vibration is Δ(unidentate) > Δ(bridging bidentate) > Δ(chelating bidentate) according to the IR data. Both **1** and **2** display blue fluorescent emission, indicating that they are potentially luminescent materials. The magnetic studies in the range 300–1.8 K indicate that complex **2** displays the characteristics of a weak antiferromagnetic coupling between metal ions in the system mediated by both types of bridging ligands between the Mn^{II} ions. Complex **2** is the first example of an open-framework coordination polymer with conjugation of blue fluorescent emission and antiferromagnetic long-range ordering, a promising candidate for multifunctional materials, such as luminescent molecular magnetic materials.

Experimental Section

Materials and Methods: 2,2′-(1,3-Phenylenedioxy)bis(acetatic acid) was prepared according to a literature method;[10c] other reagents were commercially available and used without further purification.

Synthesis of $[Zn(pdoa)(bipy)]_n$ (1): A mixture of $ZnCl_2$ (0.07 g, 0.5 mmol), 4,4′-bipyridine (0.078 g, 0.5 mmol), 2,2′-(1,3-phenylenedioxy)bis(acetic acid) (0.113 g, 0.5 mmol), methanol (10 mL), and H_2O (10 mL) was placed in a 25-mL Teflon-lined autoclave and heated to 120 °C for 72 h. Then the solution was cooled to room temperature and prismatic yellow crystals were obtained, which were filtered and washed with water and air-dried. Yield (based on $ZnCl_2$): 0.0141 g (20.1%). $C_{20}H_{16}N_2O_6Zn$ (445.74): C 53.89, H 3.62, N 6.28; found C 53.71, H 3.34, N 6.08.

Synthesis of $\{[Mn(pdoa)(bipy)](bipy)\}_n$ (2): Synthesized as brown block-shaped crystals in an identical manner to that of **1** with manganese(II) acetate tetrahydrate (0.122 g, 0.5 mmol) in place of $ZnCl_2$. Yield [based on $Mn(CH_3COO)_2 \cdot 4H_2O$]: 0.020 g (16.4%). $C_{30}H_{24}MnN_4O_6$ (591.47): C 60.92, H 4.09, N 9.47; found C 60.71, H 3.82, N 9.23.

Physical Measurements: Elemental analyses were carried out with a PE-2400CHN analyzer. The IR spectra were recorded with a Bruker VECTOR22 FTIR spectrometer in KBr pellets. Fluorescence measurements were performed with an AMINCO-Bowman Series AB_2 Luminescence Spectrometer. EPR spectra were measured with a Bruker EMX 10/12 EPR spectrometer. Magnetic susceptibility data on a crushed polycrystalline sample of **2** were collected over a temperature range of 300–1.8 K using a Quantum Design MPMS-XL superconducting quantum interference device (SQUID) magnetometer and diamagnetic corrections were made using Pascal's constants. The specific heat measurements were performed using a Quantum Design PPMS Heat Capacity System in the temperature range 300–1.8 K.

X-ray Data Collection and Structure Determination: Suitable single crystals of complexes **1** and **2** were mounted on a Pyrex fiber with

epoxy and affixed to a brass pin for the X-ray experiment. The intensity data were collected at room temperature with a Bruker Smart Apex CCD diffractometer with graphite-monochromated Mo-K_α radiation (λ = 0.71073 Å). The data were collected over a hemisphere of the reciprocal space by a combination of three sets of exposures; each set had a different φ angle (0°, 88°, and 180°) for the crystal and each exposure of 30 s covered 0.3° in ω. The crystal–detector distance was 4 cm and the detector swing angle was –35°. Coverage of the unique set was over 99% complete. The 30 initial frames were recollected at the end of data collection to monitor crystal decay by analyzing the duplicate reflections, but no significant decays were observed. The raw data collected were reduced and corrected for Lorentz and polarization effects using the SAINT program and for absorption using the SADABS program.[27] The structures were solved by direct methods using SHELXS 97[28a] and all the non-hydrogen atoms were refined anisotropically by full-matrix least squares based on F^2 values.[28b] The largest residual density peak was close to the metal atom. Hydrogen atoms were added geometrically and were not refined. CCDC-294484 (for **1**) and -294485 (for **2**) contain the supplementary crystallographic data for this paper. These data can be obtained free of charge from The Cambridge Crystallographic Data Center via www.ccdc.cam.ac.uk/data_request/cif.

Acknowledgments

We thank Prof. Manfred Scheer for his helpful suggestions and acknowledge support for this work from Jiangsu Planned Projects for Postdoctoral Research Funds, the Talent Development Foundation of Nanjing University, the Twenty-First Century Talent Foundation of the Ministry of Education, the Foundation for the Returnee of the Ministry of Education, and the Measurement Foundation of Nanjing University and the National Natural Science Foundation of China (No. 20301010).

[1] a) S. Kitagawa, R. Kitaura, S. Noro, *Angew. Chem. Int. Ed.* **2004**, *43*, 2334–2375; b) O. M. Yaghi, M. O'Keeffe, N. W. Ockwig, H. K. Chae, M. Eddaoudi, J. Kim, *Nature* **2003**, *423*, 705–714; c) C. N. R. Rao, S. Natarajan, R. Vaidhyanathan, *Angew. Chem. Int. Ed.* **2004**, *43*, 1466–1496.

[2] a) M. Eddaoudi, J. Kim, N. Rosi, D. Vodak, J. Wachter, M. O'Keeffe, O. M. Yaghi, *Science* **2002**, *295*, 469–472; b) B. Moulton, M. J. Zaworotko, *Chem. Rev.* **2001**, *101*, 1629–1658.

[3] G. Férey, *Chem. Mater.* **2001**, *13*, 3084–3098.

[4] L. Pan, K. M. Adams, H. E. Hernandez, X. Wang, C. Zheng, Y. Hattori, K. Kaneko, *J. Am. Chem. Soc.* **2003**, *125*, 3062–3067.

[5] a) J. Li, H. Zeng, J. Chen, Q. Wang, X. Wu, *Chem. Commun.* **1997**, 1213–1214; b) C. Seward, W.-L. Jia, R.-Y. Wang, G. D. Enright, S. Wang, *Angew. Chem. Int. Ed.* **2004**, *43*, 2933–2939 and references cited therein.

[6] a) L. G. Beauvais, J. R. Long, *J. Am. Chem. Soc.* **2002**, *124*, 12096–12097; b) Z. Wang, B. Zhang, H. Fujiwara, H. Kobayashi, M. Kurmoo, *Chem. Commun.* **2004**, 416–417.

[7] a) J. Bai, A. V. Virovets, M. Scheer, *Angew. Chem. Int. Ed.* **2002**, *41*, 1737–1740; b) J. Bai, J. Zuo, W. Ji, W. Tan, Z. Shen, X. You, H. K. Fun, K. Chinmakaly, I. A. Razak, *J. Mater. Chem.* **1999**, *9*, 2419–2423; c) Y. Yang, Y. Li, J. Wei, X. You, T. Wang, J. Bai, *Chin. J. Inorg. Chem.* **2004**, *20*, 683–687.

[8] Y. Q. Zheng, J. L. Lin, Z. P. Kang, *Inorg. Chem.* **2004**, *43*, 2590–2596.

[9] D.-S. Li, Y.-Y. Wang, X.-J. Luan, P. Liu, C.-H. Zhou, H.-R. Ma, Q.-H. Shi, *Eur. J. Inorg. Chem.* **2005**, 2678–2684.

[10] a) JP 04173764[92,173,764]; b) J. W. Liu, L. H. Huo, S. Gao, H. Zhao, Z. B. Zhu, J. G. Zhao, *Chin. J. Inorg. Chem.* **2004**, *20*, 707–710; c) J.-F. Zhang, Y.-H. Hu, D.-Z. Wang, *J. Cent. South Univ. Technol. (Engl. Ed.)* **2001**, *32*, 146–149.

[11] a) G. Zhang, G. Yang, J. S. Ma, *Cryst. Growth Des.* **2006**, *6*, 375–381; b) J. Tao, M.-L. Tong, J.-X. Shi, X.-M. Chen, S. W. Ng, *Chem. Commun.* **2000**, 2043–2044; c) J. Tao, J.-X. Shi, M.-L. Tong, X.-X. Zhang, X.-M. Chen, *Inorg. Chem.* **2001**, *40*, 6328–6330.

[12] J. Tao, M.-L. Tong, X.-M. Chen, *J. Chem. Soc., Dalton Trans.* **2000**, 3669–3674.

[13] a) G. R. Desiraju, *Acc. Chem. Res.* **1996**, *29*, 441–449; b) J. W. Steed, J. L. Atwood, *Supramolecular Chemistry*, John Wiley & Sons, Chichester, **2000**, p. 26.

[14] a) T. K. Maji, S. Sain, G. Mostafa, T.-H. Lu, J. Ribas, M. Monfort, N. R. Chaudhuri, *Inorg. Chem.* **2003**, *42*, 709–716; b) C. S. Hong, Y. Do, *Inorg. Chem.* **1997**, *36*, 5684–5685; c) Y.-Q. Zheng, J.-L. Lin, Z.-P. Kang, *Inorg. Chem.* **2004**, *43*, 2590–2596.

[15] T. M. Reineke, M. Eddaudi, M. O'Keeffe, O. M. Yaghi, *Angew. Chem. Int. Ed.* **1999**, *38*, 2590–2594.

[16] a) E. Y. Choi, Y.-U. Kwon, *Inorg. Chem.* **2005**, *44*, 538–545; b) X.-Z. Sun, Y.-F. Sun, B.-H. Ye, X.-M. Chen, *Inorg. Chem. Commun.* **2003**, *6*, 1412–1412.

[17] G. B. Deacon, R. J. Phillips, *Coord. Chem. Rev.* **1980**, *33*, 227–250.

[18] K. Nakamoto, *Infrared Spectra of Inorganic and Coordination Compounds*, 4th ed., John Wiley & Sons, New York, **1986**.

[19] a) S. G. Baca, Y. A. Simonov, N. V. Gerbeleu, M. Gdaniec, P. N. Bourosh, G. A. Timco, *Polyhedron* **2001**, *20*, 831–837; b) Y. Inomata, K. Sasaki, H. Umehara, F. S. Howell, *Inorg. Chim. Acta* **2001**, *313*, 95–99; c) Y.-M. Dai, E. Ma, E. Tang, J. Zhang, Z.-J. Li, X.-D. Huang, Y.-G. Yao, *Cryst. Growth Des.* **2005**, *5*, 1313–1315.

[20] J. Metz, O. Schneider, M. Hanack, *Spectrochim. Acta, Part A* **1982**, *38*, 1265–1273.

[21] J. Sun, W. Xie, L. Yuan, K. Zhang, Q. Wang, *Mater. Sci. Eng., B* **1999**, *64*, 157–160.

[22] a) C. Kutal, *Coord. Chem. Rev.* **1990**, *99*, 213–252; b) J.-H. Yang, W. Li, S.-L. Zheng, X.-M. Chen, *Aust. J. Chem.* **2003**, *56*, 1175–1178; c) R. Bertoncello, M. Bettinelli, M. Cassrin, A. Gulino, E. Tondello, A. Vittadini, *Inorg. Chem.* **1992**, *31*, 1558–1565; d) W. Chen, J.-Y. C. Chen, Q. Yue, H.-M. Yuan, J.-S. Chen, S.-N. Wang, *Inorg. Chem.* **2003**, *42*, 944–946.

[23] a) L. E. Orgel, *J. Chem. Phys.* **1955**, *23*, 1004–1014; b) S. Fernandez, J. L. Mesa, J. L. Pizarro, L. Lezama, M. I. Arriortua, R. Olazcuaga, T. Rojo, *Chem. Mater.* **2000**, *12*, 2092–2098.

[24] R. Cortés, M. Drillon, X. Solans, L. Lezama, T. Rojo, *Inorg. Chem.* **1997**, *36*, 677–683.

[25] a) K. Kopinga, T. de Neef, W. J. M. de Jonge, *Phys. Rev. B* **1975**, *11*, 2364–2369; b) J. W. Stout, E. Catalano, *J. Chem. Phys.* **1955**, *23*, 2013–2022; c) W. O. J. Boo, J. W. Stout, *J. Chem. Phys.* **1976**, *65*, 3929–3934; d) W. J. M. de Jonge, C. H. W. Swuste, K. Kopinga, K. Takeda, *Phys. Rev. B* **1975**, *12*, 5858–5863.

[26] H. Kumagai, K. W. Chapman, C. J. Kepert, M. Kurmoo, *Polyhedron* **2003**, *22*, 1921–1927.

[27] *SMART* (Version 5.0), *SAINT-plus* (Version 6), *SHELXTL* (Version 6.1) and *SADABS* (Version 2.03), Bruker AXS Inc., Madison, WI, USA, **2000**.

[28] a) G. M. Sheldrick, *SHELXS-97, Program for X-ray Crystal Structure Solution*, University of Göttingen, Göttingen, Germany, **1997**; b) G. M. Sheldrick, *SHELXL-97, Program for X-ray Crystal Structure Refinement*, University of Göttingen, Göttingen, Germany, **1997**.

Received: March 3, 2006
Published Online: July 31, 2006

